Impact of Aromatic Residues within Transmembrane Helix 6 of the Human Gonadotropin-Releasing Hormone Receptor upon Agonist and Antagonist Binding†

Sascha Hövelmann,‡ Silke H. Hoffmann,‡ Ronald Kühne,§ Ton ter Laak,|| Helmut Reiländer,⊥,# and Thomas Beckers*,‡

Department of Cancer Research, ASTA Medica AG, Weismüllerstrasse 45, D-60314 Frankfurt/Main, Germany, Institute of Molecular Pharmacology, Alfred-Kowalke-Strasse 4, D-10315 Berlin, Germany, Farmacochemie, Division of Chemistry, Vrije Universiteit Amsterdam, De Boelelaan 1083, NL-1081 HV Amsterdam, The Netherlands, and Department of Molecular Membrane Biology, Max Planck Institute of Biophysics, Heinrich-Hoffmann-Strasse 7, D-60528 Frankfurt/Main, Germany

Received June 22, 2001; Revised Manuscript Received September 26, 2001

ABSTRACT: To investigate the impact of aromatic residues within transmembrane helix 6 (TMH6) of the human gonadotropin-releasing hormone receptor (GnRH-R) on agonist and antagonist binding, residues Y^{283}, Y^{284}, W^{289}, Y^{290}, W^{291}, and F^{292} were exchanged to alanine and analyzed comprehensively in functional reporter gene and ligand binding assays. Whereas receptor mutants Y^{283}A, Y^{284}A, and W^{291}A were capable of neither ligand binding nor signal transduction, mutants W^{289}A, Y^{290}A, and F^{292}A were functional: the F^{292}A mutant behaved like wild-type receptor, while mutants W^{289}A and Y^{290}A differentiated between agonistic and antagonistic ligands. On the basis of the high-resolution X-ray structure of bovine rhodopsin as well as available data on GnRH-R mutants, models for ligand−receptor interactions are proposed. The model for D-Trp^6-GnRH (Triptorelin) binding, representing a superagonistic ligand, is in full accordance to available data. Furthermore, new interactions are proposed: $pGlu^1$ interacts with N^{212} in transmembrane helix 5, Tyr^5 with Y^{290}, and D-Trp^6 with W^{289}. The binding behavior of mutants W^{289}A and Y^{290}A corresponds to the proposed binding model for the antagonist Cetrorelix. In summary, our data as presented indicate that Y^{290} plays a key function in agonist but not antagonist binding.

Gonadotropin-releasing hormone (GnRH),[1] a decapeptide synthesized by gonadotropic cells of the hypothalamus, is a central mediator of the human reproductive axis. GnRH interacts with specific receptors on cells of the anterior pituitary gland, thereby stimulating the biosynthesis and release of LH and FSH, which promote gonadal steroid synthesis and gametogenesis (*1*). For treatment of sex hormone-dependent diseases such as precocious puberty, endometriosis, and prostate cancer, superagonistic GnRH analogues such as D-Trp^6-GnRH/Triptorelin (Decapeptyl) and D-Ser(tBu)^6-GnRH/Buserelin (Suprecure) as well as antagonists such as Cetrorelix (Cetrotide), Ganirelix (Orgalutran), and Abarelix have been developed (*2*−*6*).

The heptahelical GnRH receptor (GnRH-R) is a member of the large rhodopsin-like family of G-protein-coupled receptors (GPCRs) and has been successfully cloned from several mammalian species (*7*, *8*). Mammalian GnRH-Rs possess several unique features such as the absence of a cytoplasmic carboxy-terminal tail, the replacement of Y by S^{140} in the conserved DRY sequence in TMH3, and the reciprocal interchange of two residues highly conserved among GPCRs, namely, N^{87} in TMH2 and D^{319} in TMH7, indicating a close proximity of TMH2 and TMH7[2] (*8*). GnRH-R signal transduction depends to a large degree on the availability of G-proteins in the cellular microenvironment (*9*, *10*). It has been reported that GnRH-R couples to G_q/G_{11} but may also interact with G_i and G_s in rat pituitary cells (*11*, *12*).

To date, the bovine rhodopsin crystal structure is the only GPCR known at high resolution of 2.8 Å (*13*). Therefore, structure−function relationships in most cases rely on site-specific receptor mutants (*14*). For the GnRH-R, various receptor mutants and molecular models have been proposed. Flanagan et al. showed that residue D^{98} of the human GnRH-R has a dual function by forming a TMH2−TMH3 interhelical ionic interaction with K^{121} and interacting via a

† This work was supported by the Federal Ministry of Research, Education, Science, and Technology (BMBF), Grant 0310697A to ASTA Medica AG and R.K.

* To whom correspondence and reprint requests should be addressed. E-mail: T.Beckers@vff.uni-frankfurt.de. Phone: +49 69 4001 2822. Fax: +49 69 4001 2777.

‡ ASTA Medica AG.

§ Institute of Molecular Pharmacology.

|| Vrije Universiteit Amsterdam.

⊥ Max Planck Institute of Biophysics.

Present address: Aventis Pharma AG, Industriepark Hoechst, Building H811, D-65926 Frankfurt/Main, Germany.

[1] Abbreviations: Cit, citrulline; CMV, cytomegalovirus; Cpa, 3-(4-chlorophenyl)alanine; CRE, cAMP-responsive element; DMEM, Dulbecco's modified Eagle's medium; EL, extracellular loop; FCS_i, heat-inactivated fetal calf serum; FSH, folicle stimulating hormone; GnRH, gonadotropin-releasing hormone; GnRH-R(s), gonadotropin-releasing hormone receptor(s); GPCR, G-protein-coupled receptor; IL, intracellular loop; LH, luteinizing hormone; Luc, firefly luciferase; Nal, 3-(2-naphthyl)alanine; Pal, 3-(3-pyridyl)alanine; RLU, relative light units; SEAP, placental-type secreted alkaline phosphatase; tBu, *tert*-butyl; TMH, transmembrane helix.

[2] The GnRH-R residues in this paper are numbered according to the human GnRH-R protein sequence. Mouse and rat GnRH-R lack residue K^{191} of the human receptor, causing a shift by −1 starting with V^{191} (*31*, *32*).

10.1021/bi0113162 CCC: $22.00
Published on Web 01/03/2002

hydrogen bond with the δ-NH group of His^2 of GnRH (*15*). Direct interactions of N^{102} (TMH2) and D^{302} (EL3/TMH7) with the ligand were demonstrated and are proposed for W^{101} (TMH2), K^{121} (TMH3), N^{212} (TMH5), and W^{280} (TMH6) (*15*−*20*). New studies gave hints to the importance of TMH6, since residues in proximity to and within intracellular loop 3 are important for receptor signaling, and residues close to the extracellular side of TMH6 are supposed to be involved in agonist binding. Mutants within intracellular loop 3 ($R^{262}Q$) and TMH6 ($Y^{284}C$) discovered in patients with idiopathic hypogonadotropic hypogonadism (IHH) exhibited only marginal influence on ligand binding, while the activation of phospholipase C was considerably affected (*21*, *22*). The aromatic character of residue F^{276} in TMH6 is important for receptor expression as well as ligand binding, while mutation of W^{279} (rat GnRH-R) to S or R resulted in a significant reduction or total loss of ligand binding (*20*, *23*).

Modeling experiments suggested that residues within TMH6 contribute to the formation of a deep hydrophobic binding pocket (*19*, *20*). On the basis of these findings, the present study evaluated the effects of substituting aromatic residues Y^{283}, Y^{284}, W^{289}, Y^{290}, W^{291}, and F^{292} in TMH6 for alanine. After selection of cell lines stably expressing the single receptor mutants, agonist and antagonist binding as well as signaling capacity were analyzed. As revealed by this analysis, the receptor residue Y^{290} is highly important for agonist but not antagonist binding. Refined molecular models for binding of Triptorelin and Cetrorelix based on the rhodopsin structure are presented and discussed in the context of the receptor mutant data.

MATERIALS AND METHODS

Recombinant DNA Procedures and Site-Specific Mutagenesis. Standard methods for recombinant DNA were applied (*24*). Site-specific mutagenesis was carried out according to the Clontech Transformer site-directed mutagenesis manual and as has been described previously (*19*). The Trans Oligo *Alw*NI/*Spe*I (Clontech Laboratories, Inc., Palo Alto, CA) was used as a selection primer, whereas mutagenesis primers were as follows: Y^{283}A, 5′-GCTGGACTCCCGCATATGTC-CTAG G-3′; Y^{284}A, 5′-GGACTCCCTACGCGGTCCTAG-GAAT TTG-3′; W^{289}A, 5′-GTCCTAGGAATCGCGTAT-TGGTTTGATCC-3′; Y^{290}A, 5′-CTAGGAATTTGGGCCT-GGTTTGATCC-3′; W^{291}A, 5′-GGAATTTGGTATGCATTT GATCCTG-3′; F^{292}A, 5′-GAATTTGGTATTGGGCCGATC-CTGAAATG- 3′.

The dicistronic vector pSBC mt hGnRHR/IRES/SEAP was obtained by *Ase*I/*Not*I fragment shuffling between the pSBC1-hGnRHR and pSBC2-IRES-SEAP. Mutations were verified by restriction enzyme analysis and DNA sequencing.

Mammalian Cell Culture, Stable Transfection, and Selection of Cell Clones. Murine thymidine kinase deficient L cells (LTK^-) and transfectants thereof were cultured at 37 °C and 5% CO_2 in Dulbecco's modified Eagle's medium (DMEM) supplemented with 10% inactivated fetal calf serum (FCS_i), penicillin/streptomycin, and glutamine. The clonal cell line 122 was chosen as the reporter cell line for stable supertransfection with the human GnRH-R mutants as described (*19*). All functional or binding assays were performed with cell pools at low passage number and under G418 selection, since receptor expression markedly decreased during passages.

Agonistic and Antagonistic GnRH Analogues and Luciferase Reporter Gene Assay. Cetrorelix/D-20761 (Ac-D-Nal^1-D-Cpa^2-D-Pal^3-Ser^4-Tyr^5-D-Cit^6-Leu^7-Arg^8-Pro^9-D-Ala^{10}-NH_2) and Antarelix/D-23234 (Ac-D-Nal^1-D-Cpa^2-D-Pal^3-Ser^4-Tyr^5-D-Hci^6-Leu^7-$Lys(^iPr)^8$-Pro^9-D-Ala^{10}-NH_2) were synthesized by ASTA Medica AG, Frankfurt, Germany (*4*). Agonistic peptides GnRH, des-Gly^{10}-Pro-$NHEt^9$-GnRH, D-Trp^6-GnRH, des-Gly^{10}-D-Trp^6-Pro-$NHEt^9$-GnRH, D-Ala^6-GnRH, and des-Gly^{10}-D-Ala^6-Pro-$NHEt^9$-GnRH were purchased from Bachem Biochemica GmbH, Heidelberg, Germany. All peptides except of Cetrorelix, which was dissolved in 0.01 N CH_3-COOH, were dissolved in H_2O at 1 mM final concentration and stored in siliconized polypropylene tubes at −20 °C.

Functional Reporter Gene and Radioligand Binding Assays. The functional analysis of the receptor mutants was performed in 96-well microtiter plates as described earlier (*19*). For determination of antagonistic potency, cells were preincubated for 15 min with Cetrorelix or Antarelix prior to stimulation with D-Trp^6-GnRH. Variable D-Trp^6-GnRH concentrations of $2 \times EC_{50}$ were used for stimulation, depending on the GnRH-R mutant tested. EC_{50} and IC_{50} values were calculated by nonlinear regression analysis using the Hill model, and mean values ± SD (sample deviation σ_{n-1}) from at least two independent experiments are shown.

For displacement binding experiments, [^{125}I]Cetrorelix was used as a tracer. This radioligand is superior to agonists such as [^{125}I]Triptorelin in terms of high binding affinity and ≥80% of tracer capable for specific receptor association. Thus, it was possible to determine dissociation constants for receptor mutants with decreased expression or binding affinity. The assay was carried out under physiological conditions with intact cells as described (*19*, *30*). Briefly, 1×10^6 cells/100 μL were incubated for 1 h at 37 °C with ~225 pM [^{125}I]Cetrorelix [specific activity $(5-10) \times 10^5$ dpm/pmol] and different concentrations of unlabeled Cetrorelix as a competitor. Using the EBDA/Ligand analysis program (Biosoft V3.0, Cambridge, U.K.), the dissociation constant (K_D) and cell surface receptor expression (B_{max} in picomolar) were calculated. Mean values ± SD (sample deviation σ_{n-1}) from at least two independent experiments are shown.

Molecular Modeling Experiments. The starting structure for the TMHs of the human GnRH-R was built from the human receptor protein (SwissProt P30968) by using the X-ray structure of bovine rhodopsin as a template (*13*). The extra- and intracellular domains of the human GnRH-R were built by combination of de novo homology modeling based on three-dimensional structures of sequence elements using the Brookhaven database and Cα positions derived from the rhodopsin structure for more conserved sequences. Two disulfide bridges were included into the model; the highly conserved disulfide bridge $C^{114}-C^{196}$ was located at the same place as in the rhodopsin structure (*13*, *35*). The disulfide bridge $C^{14}-C^{200}$ stabilizes the antiparallel β-strands formed by the second EL and the N-terminus (*27*). To avoid van der Waals clashes, this starting structure was minimized using the sander module of AMBER5.0 up to an energy gradient less than 0.05 (*28*). As in earlier studies dealing with TMH stability, positively charged R and K and negatively charged E and D residues were used (*29*). The minimized receptor model was refined by repeated simulated annealing molecular dynamics using AMBER5.0 (20 runs, in vacuo, heating to 1500 K within 5 ps, followed by a hot phase of 20 ps and

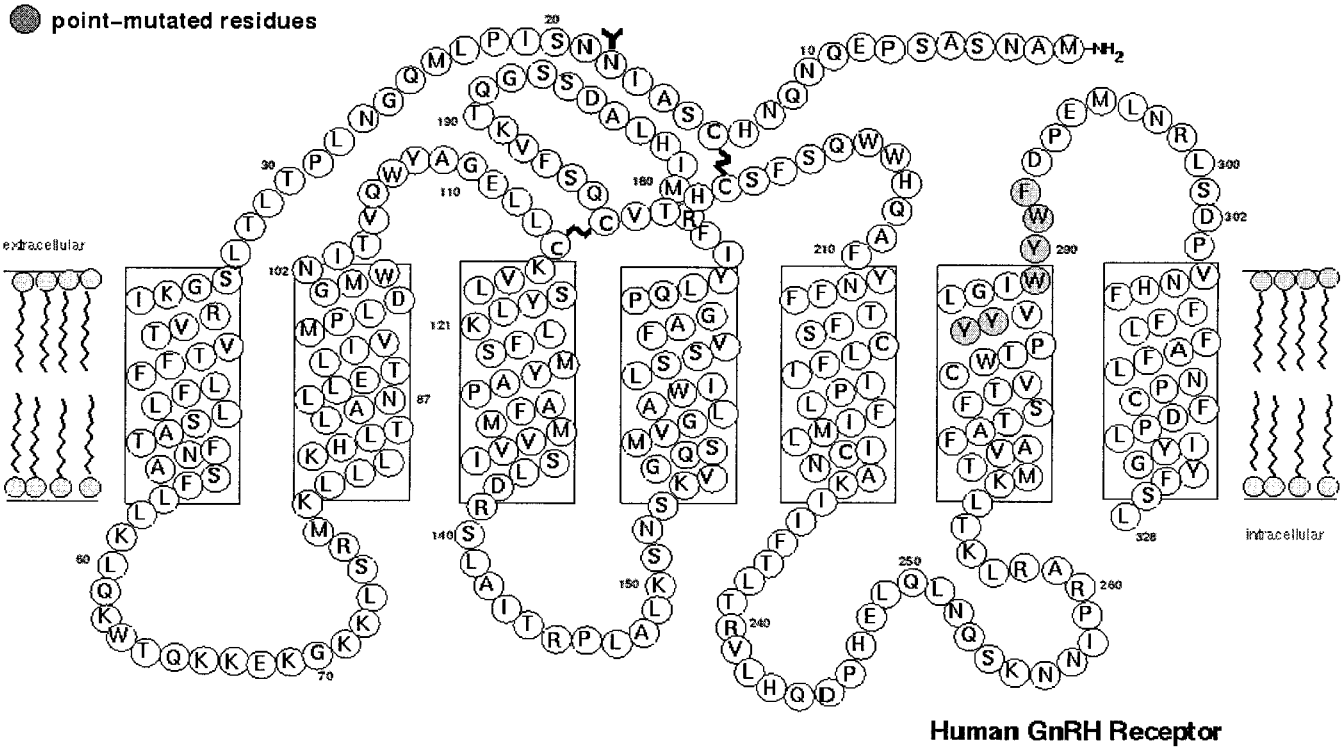

FIGURE 1: Schematic view of the human GnRH-R. A simplified model of the human GnRH-R with the putative N-glycosylation site (N^{18}) and disulfide bonds between C^{14}−C^{200} and C^{114}−C^{196} is presented (*27, 31*−*35*). Mutated aromatic residues in TMH6, namely, Y^{283}, Y^{284} W^{289}, Y^{290}, W^{291}, and F^{292}, are highlighted.

finally slowly cooling to 0 K over 25 ps, using harmonic restraint on all Cα atoms of 1 kcal mol^{-1} $Å^{-2}$). To choose the best model, the quality of the generated structures was evaluated using the ProCheck program (version 3.5). The structure with the highest score (overall average of *G*-factor −0.42) in combination with the lowest unconstraint Amber energy was selected for all further studies.

Starting from about 30 Å outside the GnRH-R pocket, D-Trp^6-GnRH was docked into the putative agonist binding site during 100 ps of AMBER5.0 molecular dynamics simulation (in vacuo, 300 K, 9 Å nonbonded cutoff, 2 fs step width, using shake option to constraint the bond lengths involving hydrogen). The centers of mass of interacting amino acid residues identified experimentally [$pGlu^1$ with N^{212} (*19*), Arg^8 with D^{302} (*18*), His^2 with D^{98} (*15*), Gly^{10}-NH_2 with N^{102} (*17*), and D-Trp^6 close to C^{14} (*27*)] were restrained to gradually approach a distance smaller than 3.5 Å or 8 Å for the D-Trp^6−C^{14} interaction. During the simulation, the Cα atoms of the receptor were restricted using harmonic restraints of 1 kcal mol^{-1} $Å^{-2}$ that allow only small conformational changes of the receptor model. In the case of Cetrorelix, the same docking procedure was performed using hypothetical interaction maps (N-terminal acetyl group with N^{212}, D-Cit^6 with C^{14}, Arg^8 with D^{302}, and D-Ala^{10}-NH_2 with N^{102}, center of mass for Cα atoms of D-Nal^1, D-Cpa^2, and D-Pal^3 close to W^{280}). Except for the center of mass−W^{280} interaction (8 Å), the restraints were defined to reach 3.5 Å after simulation.

To generate different ligand binding modes, repeated simulated annealing was applied. Using different sets of restraints to test various hypotheses on binding modes, 320 simulated annealing runs for the D-Trp^6-GnRH receptor interaction were calculated representing eight different sets of intermolecular restraints, while 200 simulated annealing runs (five different restraint sets) for Cetrorelix binding mode were performed. After minimization, the binding models as obtained were ranked according to the calculated binding energies. Models having the highest ligand binding energies were selected, and the effect of Y^{283}A, Y^{284}A, W^{289}A, Y^{290}A, W^{291}A, and F^{292}A mutants on ligand binding energy was calculated for each of these models. Binding models which were in best accordance to experimental and calculated ligand binding energies were selected.

RESULTS

Site-Specific Mutants of the Human GnRH-R. As TMH6 of the human GnRH-R is supposed to significantly contribute to the formation of the hydrophobic ligand binding pocket, receptor residues Y^{283}, Y^{284}, W^{289}, Y^{290}, W^{291}, and F^{292} were substituted for alanine by site-specific mutagenesis (Figure 1). After stable expression of the mutant receptor proteins, displacement binding and functional reporter gene studies were performed by using intact cells under physiological conditions. Functional data were raised with GnRH and the agonistic analogues D-Trp^6-GnRH, des-Gly^{10}-Pro-$NHEt^9$-GnRH, des-Gly^{10}-D-Trp^6-Pro-$NHEt^9$-GnRH, D-Ala^6-GnRH, and des-Gly^{10}-D-Ala^6-Pro-$NHEt^9$-GnRH or the antagonists Cetrorelix and Antarelix.

Ligand Binding toward Human GnRH-R Mutants. Homologous displacement binding studies were performed with [^{125}I]Cetrorelix as a superior radioligand regarding high specific activity and long stability. From these studies it became evident that binding of Cetrorelix to cells transfected with receptor mutants Y^{283}A, Y^{284}A, and W^{291}A was below detection level. In contrast, receptor mutants W^{289}A, Y^{290}A,

Table 1: Summary of Data Derived from Functional and Displacement Binding Experiments for GnRH-R Mutants[a]

		receptor mutant			
		wt	$W^{289}A$	$Y^{290}A$	$F^{292}A$
activation of signal transduction by agonists, EC_{50} (nM)	GnRH	2.2 ± 0.2 (3) **1.0**	34 ± 4.5 (5) **16**	1600 ± 500 (6) **730**	5.6 ± 1.9 (4) **2.5**
	des-Gly^{10}-Pro-NHEt^{9}-GnRH	0.47 ± 0.13 (4) **1.0**	2.3 ± 0.9 (5) **4.9**	470 ± 140 (2) **1000**	1.5 ± 0.2 (4) **3.2**
	D-Trp^{6}-GnRH	0.75 ± 0.05 (6) **1.0**	4.4 ± 2.1 (5) **5.9**	150 ± 80 (5) **200**	2.7 ± 1.5 (6) **3.6**
	D-Ala^{6}-GnRH	0.95 ± 0.14 (6) **1.0**	7.7 ± 1.5 (4) **8.1**	690 ± 50 (2) **730**	1.6 ± 0.2 (4) **1.7**
	D-Ala^{6}-des-Gly^{10}-Pro-NHEt^{9}-GnRH	0.45 ± 0.01 (2) **1.0**	3.6 ± 0.5 (4) **8.0**	180 (1) **400**	0.80 ± 0.09 (4) **1.8**
inhibition of signal transduction by antagonists, IC_{50} (nM)	Cetrorelix	1.1 ± 0.2 (3) **1.0**	2.0 ± 0.4 (4) **1.8**	4.0 ± 1.4 (3) **3.6**	3.4 ± 0.7 (4) **3.1**
	Antarelix	1.4 ± 0.3 (4) **1.0**	5.2 ± 1.9 (6) **3.7**	3.5 ± 0.8 (3) **2.6**	7.1 ± 2.0 (6) **5.1**
displacement binding with [^{125}I]Cetrorelix	K_D (nM)	0.21 ± 0.07 (4) **1.0**	0.43 ± 0.19 (3) **2.1**	0.28 ± 0.11 (2) **1.3**	0.39 ± 0.22 (4) **1.9**
	B_{max} (pM)	8.3 ± 5.3 (4) **1.0**	2.1 ± 0.6 (3) **0.25**	1.9 ± 0.5 (2) **0.23**	3.1 ± 1.0 (4) **0.37**
maximal activation of signal transduction by D-Trp^{6}-GnRH	E_{max} (rlu)	28521 ± 3368 (8) **1.0**	5472 ± 1872 (8) **0.19**	5118 ± 1958 (8) **0.18**	12964 ± 2710 (8) **0.46**

[a] The alanine mutants of residues Y^{283}, Y^{284}, and W^{291} neither bound ligand nor showed agonist-induced signal transduction. Binding affinity K_D and cell surface expression B_{max} for receptor mutants $W^{289}A$, $Y^{290}A$, and $F^{292}A$ were determined in displacement binding experiments with [^{125}I]Cetrorelix; EC_{50} and E_{max} values were calculated from functional assays with different agonistic ligands; IC_{50} values were calculated from functional assays with D-Trp^{6}-GnRH as the agonistic stimulus (for details see Materials and Methods). The EC_{50}, IC_{50}, K_D, B_{max}, and E_{max} values obtained for the mutant GnRH-Rs were divided by that of the wild-type receptor. The resulting indices for ligand binding (affinity/K_D), surface expression (stability/B_{max}), or receptor activation (activity/EC_{50} and IC_{50}) are printed in boldface. Mean values ± SD from independent experiments (numbers in parentheses) are shown.

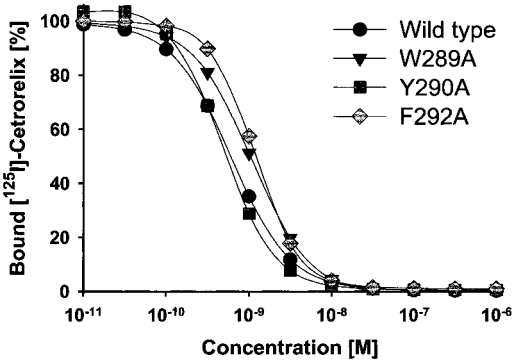

FIGURE 2: Binding affinity of GnRH-R mutants toward Cetrorelix. Cell pools stably expressing receptor mutants $W^{289}A$, $Y^{290}A$, and $F^{292}A$ were analyzed in homologous displacement binding experiments with [^{125}I]Cetrorelix. Dose−response curves of typical experiments are shown (see Table 1 for further details).

and $F^{292}A$ were capable of ligand binding, and the dissociation constants K_D as well as B_{max} values for binding affinity and cell surface expression, respectively, were calculated from displacement binding curves (Figure 2 and Table 1). Compared to the wild-type receptor, binding affinities and expression of mutant proteins were decreased (Table 1). Taking into account that a polyclonal cell population was evaluated, GnRH-R expression was low but within the range of expression determined in heterogeneous cell populations (*30*).

Signaling Capacity of GnRH-R Mutants. Consistent with the displacement binding experiments, agonist-induced signaling of cells transfected with receptor mutants $Y^{283}A$, $Y^{284}A$, and $W^{291}A$ was below detection level. In contrast, signal transduction was observed for mutants $W^{289}A$, $Y^{290}A$, and $F^{292}A$. Dose−response curves were typically sigmoid-shaped and highly reproducible as represented in Figure 3 and summarized in Table 1 for GnRH, D-Trp^{6}-GnRH, and the antagonists Cetrorelix and Antarelix. The IC_{50} values for Cetrorelix as determined were in good accordance to the K_D values, and we assumed that the mutations affected ligand binding, while signal transduction was only affected as a consequence. To facilitate the data interpretation, the EC_{50}, IC_{50}, K_D, B_{max}, and E_{max} values obtained for the mutant GnRH-Rs were divided by that of the wild-type receptor. The resulting indices for activity, affinity, and expression indicate the influence of a receptor mutation on ligand binding (affinity/K_D), surface expression (stability/B_{max}), and receptor activation (activity/EC_{50}).

Substitution of residues W^{289} and Y^{290} for alanine led to mutant receptors that discriminated between agonists and antagonists. The $Y^{290}A$ mutation displayed a very strong effect on agonist-dependent receptor activation (activity index ranging from 200 to 1000; Table 1). In contrast, activity

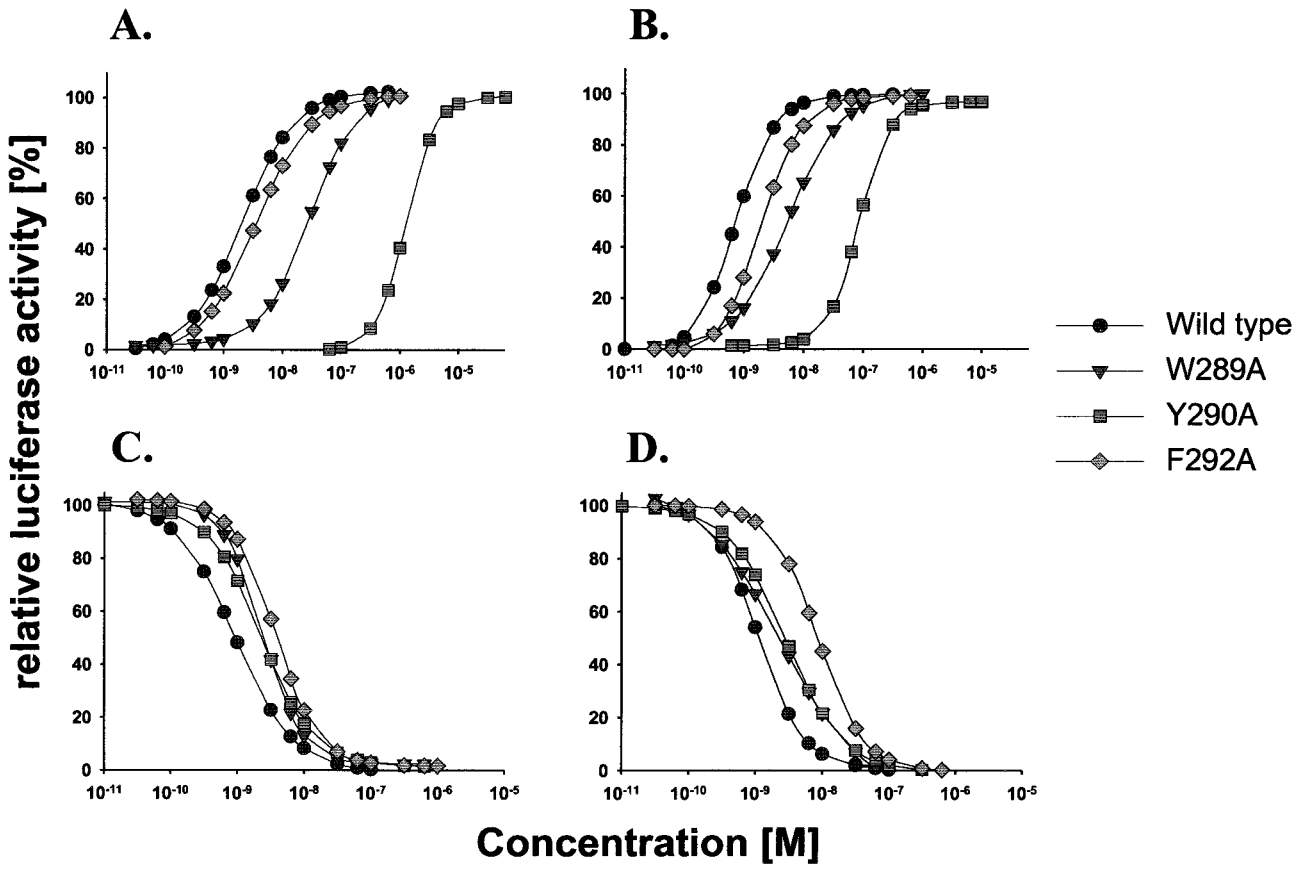

FIGURE 3: Functional characteristics of GnRH-R mutants. Mutants W^{289}, Y^{290}, and F^{292} were analyzed for receptor activation upon agonist binding and inhibition of D-Trp^6-GnRH-induced activation by antagonists. Normalized dose−response curves of typical experiments with GnRH (A), D-Trp^6-GnRH/Triptorelin (B), Cetrorelix (C), and Antarelix (D) are shown.

indices for the antagonists Cetrorelix and Antarelix with 3.6 and 2.6, respectively, were virtually identical to the wild-type receptor. Since binding affinity of Cetrorelix toward the Y^{290}A mutant with $K_D = 4.0$ nM was marginally affected, we assumed that Y^{290} is only important for agonist binding. To a certain extent this is also true for residue W^{289}, although binding of conformationally constrained agonists such as D-Trp^6-GnRH was comparable to that of antagonists. In contrast to Y^{290} and W^{289}, residue F^{292} was significantly involved in neither ligand binding nor signaling.

Cell surface expression (B_{max}) of mutant and wild-type GnRH-R proteins calculated from displacement binding experiments ranged from 1.9 pM (Y^{290}A) to 8.3 pM (wild-type), strictly correlating with E_{max} as the maximal functional response after stimulation with D-Trp^6-GnRH. We conclude that the lower E_{max} values of mutant receptors were due to reduced surface expression, which is further supported by a previous study with mutants in TMH5 (*19*).

Molecular Models for Binding of D-*Trp*^{6}*-GnRH and Cetrorelix.* By using a high-resolution template structure to model the human GnRH-R, important differences to molecular models as published became evident (*15*, *19*, *20*). In this regard the folding of the extracellular domain of rhodopsin was extremly helpful. Like rhodopsin, the GnRH-R model showed a compact extracellular domain stabilized by two disulfide bridges and the extracellular loop 2 located quite deep in the transmembrane region of the receptor. A putative ligand binding site was identified, which is located between TMH2 (E^{90}-N^{102}), TMH3 (S^{118}-Y^{126}), TMH5 (F^{216}-N^{212}), TMH6 (W^{280}-Y^{290}), TMH7 (F^{313}-D^{302}), EL2 (Q^{189}-W^{206}), and EL3 (D^{293}-E^{295}). The shape of this binding site is causative for the preference of the "horseshoe-like" conformation of bound D-Trp^6-GnRH (Figure 4A). The agonist binding mode is determined mainly by the following interactions: $pGlu^1$ hydrogen bonds to N^{212}; His^2 points toward D^{98} and K^{121}, replacing the $K^{121}-D^{98}$ interaction in the receptor without ligand; Trp^3 interacts with W^{280}; Ser^4 stabilizes the β-II-turn-like agonist conformation forming a intramolecular hydrogen bond to the backbone NH of Leu^7; Tyr^5 is located close to Y^{290}; D-Trp^6 fills a hydrophobic pocket in the extracellular domain adjacent to the second disulfide bridge ($C^{14}-C^{200}$) and W^{289}; Arg^8 forms a salt bridge with D^{302}; and the C-terminus forms hydrogen bonds to D^{98} and N^{102}.

The preferred docking mode for Cetrorelix is highlighted in Figure 4B. The N-terminal acetyl group forms a hydrogen bond with N^{212}; D-Nal^1 interacts with F^{216}; D-Cpa^2 is in close contact to W^{280}, indicating a high probability that these residues are involved in charge-transfer interactions; D-Pal^3 points toward K^{121} but does not change the $K^{121}-D^{98}$ interaction; Ser^4 participates in an intramolecular hydrogen bond to the carbonyl oxygen of the Arg^8 backbone; Tyr^5 is located close to D-Nal^1 stabilized by $\pi-\pi$ interaction and an additional intramolecular hydrogen bond to the carbonyl oxygen of the D-Cit^6 side chain; D-Cit^6 fills out the hydrophobic core adjacent to the $C^{14}-C^{200}$ disulfide bridge; Arg^8 forms a salt bridge to D^{302} and the C-terminal D-alanine^{10}-NH_2 is involved in hydrogen bonds to both N^{102} and W^{101}.

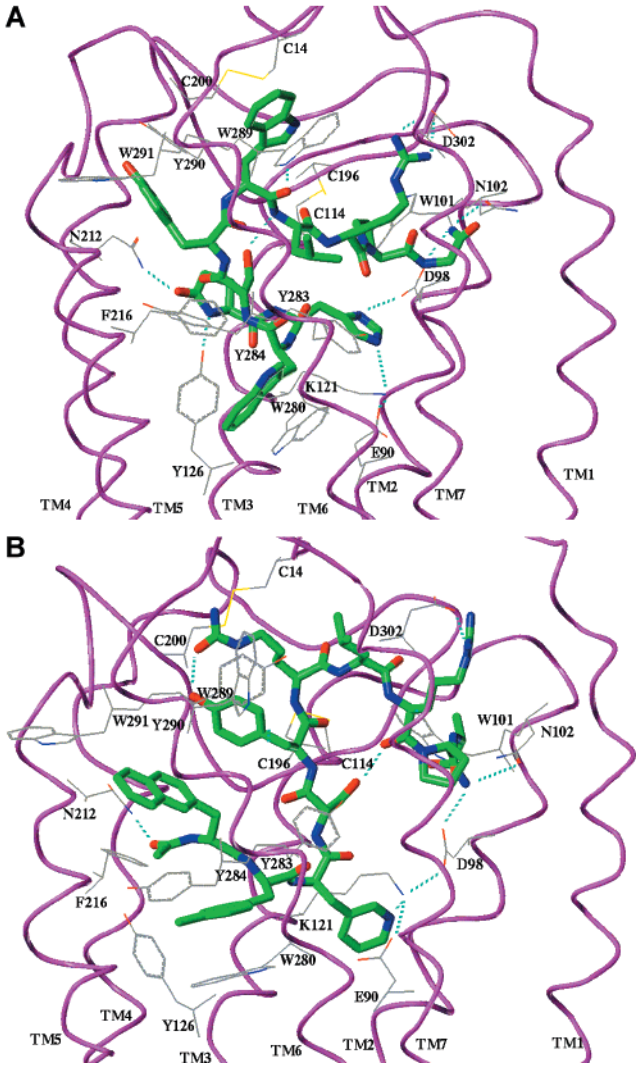

FIGURE 4: Molecular model of the ligand−receptor complex. The model of GnRH-R with agonist D-Trp^6-GnRH as the ligand (in green) is shown in (A) with the most favored agonist−receptor interactions highlighted (for details see text). The N-terminal residues pGlu^1 and His^2 bridge the gap between TMH2 and TMH5 (11.3 Å distance between pGlu^1 oxygen and ϵN-His^2). In the model, His^2 is able to interact with both K^{121} and D^{98}. This interaction changes the orientation of the K^{121} side chain from TMH2 to TMH7 and places His^2 in proximity to the C-terminus of D-Trp^6-GnRH. The model of GnRH-R with the antagonist Cetrorelix as the ligand is shown in (B). The N-terminal acetyl group forms a hydrogen bond to N^{212}, and the D-Pal^3 side chain interacts with K^{121} (for details see text). Since the distance between the acetyl−carbonyl oxygen and the pyridyl−N is increased to 13.5 Å, the orientation of the K^{121} side chain toward TMH2 is not affected. The disulfide bonds between C^{14}−C^{200} and C^{114}−C^{196} in the extracellular portion of the receptor−ligand complex are shown in yellow.

DISCUSSION

A prerequisite for the rational design of potent peptidic and peptidomimetic GnRH receptor antagonists are structure−activity-relationships (SAR) as well as models of the three-dimensional structure of the receptor binding pocket. We recently proposed a receptor model, where a deep hydrophobic ligand binding pocket was formed by TMH5, TMH6, and TMH7 with additional contributions by residues from TMH3, TMH2, and extracellular loops 2 and 3 (*19*). Within the present study, alanine mutants of aromatic residues Y^{283}, Y^{284}, W^{289}, Y^{290}, W^{291}, and F^{292} within TMH6 were evaluated after stable expression in murine L-cells for ligand binding and signal transduction properties. Transfection of alanine mutants of residues Y^{283}, Y^{284}, and W^{291} yielded cells capable of neither Cetrorelix binding nor D-Trp^6-GnRH stimulated signaling. This can be explained by destruction of the overall receptor structure and/or ligand binding pocket, failure of proper integration into the membrane, and, therefore, loss of surface expression or synthesis of misfolded protein targeted to the proteosome. The importance of residue Y^{284} has recently been discussed in idiopathic hypogonadotropic hypogonadism (IHH). Although binding of GnRH-A to the mutant Y^{284}C was normal, receptor expression and IP_3 production signaling were severly diminished (*21*).

The mutants W^{289}A, Y^{290}A, and F^{292}A, which bound ligand and were activated by agonists, were studied in detail. Residues Y^{290} and to some extent W^{289} are important for binding of agonists but not antagonists. As found in earlier studies as well, this was more pronounced for GnRH as for constrained agonists such as D-Trp^6-GnRH. Most likely, by having a predisposed β-II-turn conformation, binding of constrained agonists is less dependent on a defined receptor structure needed for binding of GnRH by an induced fit (*19*). Compared to wild-type receptor, the mutants W^{289}A, Y^{290}A, and F^{292}A were expressed at significantly lower levels. As shown previously, an effect of receptor expression levels on responsiveness is highly unlikely because receptor affinity and antagonistic potency correlate and weakly or strongly expressed mutants depicted wild-type activity (*19*). We believe that "spare receptors" as proposed by Zhou et al. (*16*) are related to massive overexpression of GnRH receptor proteins in a transient expression system. The correlation of E_{max} and B_{max} values for wild-type and mutant GnRH-R also strongly supports the notion that G-protein coupling is uneffected by either mutation, and differences in EC_{50} values are a consequence of differences in agonist binding.

On the basis of the X-ray structure of bovine rhodopsin and the receptor mutant data presented herein, we refined our GnRH-R model (*13*, *19*). Binding modes for D-Trp^6-GnRH and Cetrorelix were evaluated by repeated simulated annealing molecular dynamics calculations. The final model for D-Trp^6-GnRH as shown in Figure 4A is in full accordance to the data as presented and published recently (*15*, *19*, *20*). In the receptor model, His^2-δNH interacts with D^{98} in TMH2, and His^2 is located between D^{98} and K^{121}, stabilized by an additional hydrogen bond between ϵN-His^2 and the K^{121} side chain. The pGlu^1 residue points toward TMH5, corresponding to the domain of rhodopsin occupied by the ionone ring of retinal (*13*), interacting with N^{212}. Both pGlu^1 and His^2 are located below EL2 in proximity to TMH3, thereby changing the position of EL2 slightly to the extracellular part of the receptor. The position of pyroGlu^1-His^2 leads to an orientation of Trp^3 toward TMH6, filling a hydrophobic pocket formed by W^{280}, Y^{283}, Y^{284}, F^{216}, and Y^{126}. In addition, Y^{283} and Y^{284} participate in interhelical interactions between TMH5 and TMH6 (S^{217} with Y^{284}) and between TMH6 and TMH7 (Y^{283} with the carbonyl backbone of F^{303}). The complex interactions of Glu^1-His^2-Trp^3 lead to an orientation of Ser^4- Tyr^5-D-Trp^6 parallel to the upper part of TMH6 with Ser^4 forming a stable intramolecular hydrogen bond to the backbone NH of Leu^7, thereby stabilizing the β-II-turn-like conformation of Tyr^5-D-Trp^6. This conformation exposes the Tyr^5 side chain on the top of TMH6, making a strong

aromatic interaction with Y^{290}. This interaction prefers a Y^{290} side chain rotamer with the aromatic ring located toward the upper part of TMH5. In contrast, in the unliganded receptor model a Y^{290} side chain rotamer is preferred with the side chain close to the top of TMH7. Thus, the agonist-induced conformational change of Y^{290} opens a space filled out by W^{289}, which now is available for the aromatic interaction and formation of a hydrogen bond to the carbonyl oxygen of D-Trp^6. This cascade of ligand−receptor interactions nicely explains the experimental data for the Y^{290}A and W^{289}A mutants. The position of D-Trp^6 close to the second extracellular disulfide bridge is in agreement with data by Davidson et al. (*27*). In the receptor model, W^{291} as the third aromatic residue in the upper part of TMH6 faces the outer part of the plasma membrane. The C-terminal Arg^8-Gly^{10}-NH_2 residues do bind as proposed recently; namely, Arg^8 interacts with D^{302} and N^{102} with Gly^{10}-NH_2, stabilized by an additional hydrogen bond to D^{98} (*15*, *18*, *19*).

The receptor model for Cetrorelix binding as shown in Figure 4B is remarkably different. In the model D-Pal^3 interacts with K^{121} via a hydrogen bond. In contrast to the His^2−K^{121} interaction of the D-Trp^6-GnRH binding model, the pyridyl ring−K^{121} hydrogen bond does not change the position of the protonated nitrogen of K^{121} in the middle of D^{98} and E^{90}. The different orientation of ξN-K^{121} close to TMH2 in the antagonist binding mode and unliganded receptor model compared to the orientation of ξN-K^{121} toward TMH7 in the agonist binding mode is a hint to the molecular mechanism of receptor activation. Due to the D-Pal^3−K^{121} interaction, D-Cpa^2 can bind to W^{280} by charge-transfer interaction, occupying a hydrophobic pocket with Y^{283}, Y^{284}, F^{216}, and F^{220}. In agreement with previous data, the N-terminal acetyl group of Cetrorelix interacts with N^{212} via a hydrogen bond (*19*). In analogy to the agonist model, this interaction is stabilized by an additional hydrogen bond between the δ^1-O of N^{212} and ϵNH of W^{206}. The backbone NH of D-Nal^1 hydrogen bonds to the T^{198} side chain within the second extracellular loop in the vicinity to Cetrorelix. In contrast to our agonist binding model, the antagonist binding mode does not influence the relatively deep location of EL2, being similar to that found in the X-ray structure of dark-adapted bovine rhodopsin. The D-Nal^1 side chain contacts via hydrophobic interactions receptor residues F^{216} and F^{213} and Tyr^5 of the ligand itself. The pattern of receptor interactions with D-Nal^1-D-Cpa^2-D-Pal^3 leads to an extended backbone conformation between Ser^4 and D-Cit^6 located between TMH6, TMH7, and the extracellular loop 2. As a result, Tyr^5 is stabilized by an intramolecular hydrogen bond between the Tyr hydroxyl group and the carbonyl oxygen of the D-Cit^6 side chain. Additionally, the model shows an aromatic contact to D-Nal^1 and to some extent to Y^{290}. The intramolecular stabilization of the Cetrorelix conformation explains why the Y^{290}A mutant does not have an influence on antagonist binding. In contrast to the agonist binding mode, Y^{290} adopts a side chain rotamer making an interaction of W^{289} with Cetrorelix impossible. In the case of the Y^{290}A mutant, the W^{289} side chain can substitute for the missing aromatic contact.

In summary, the proposed models for binding of D-Trp^6-GnRH and Cetrorelix as prototypic agonistic and antagonistic ligands to the GnRH-R are in agreement with the experimental data with receptor residues W^{289} and Y^{290} involved in agonist binding only. We propose that Y^{290} has a key function in the discrimination between receptor agonists and antagonist and hence receptor activation.

ACKNOWLEDGMENT

We acknowledge the excellent assistance of E. Thoenes, M. Hartmann, and E. Uloth. We thank Dr. M. Bernd for synthesis of antagonists Cetrorelix and Antarelix. The ligand [^{125}I]Cetrorelix was prepared and kindly provided by Dr. G. P. McGregor, Philipps-Universität, Marburg, Germany.

REFERENCES

1. Evans, J. J. (1999) *Endocr. Rev. 20*, 46−67.
2. Conn, P. M., and Crowley, W. F. (1991) *N. Engl. J. Med. 324*, 93−103.
3. Emons, G., and Schally, A. V. (1994) *Hum. Reprod. 9*, 1364−1379.
4. Kutscher, B., Bernd, M., Beckers, T., Polymeropoulos, E. E., and Engel, J. (1997) *Angew. Chem. 109*, 2240−2254.
5. Gillies, P. S., Faulds, D., Balfour, J. A., and Perry, C. M. (2000) *Drugs 59*, 107−111.
6. Cook, T., and Sheridan, W. P. (2000) *Oncologist 5*, 162−168.
7. Stojilkovic, S. S., Reinhart, J., and Catt, K. J. (1994) *Endocr. Rev. 15*, 462−499.
8. Sealfon, S. C., Weinstein, H., and Millar, R. P. (1997) *Endocr. Rev. 18*, 180−205.
9. Stanislaus, D., Pinter, J. H., Janovick, J. A., and Conn, P. M. (1998) *Mol. Cell. Endocrinol. 144*, 1−10.
10. Naor, Z., Harris, D., and Shacham, S. (1998) *Front. Neuroendocrinol. 19*, 1−19.
11. Stanislaus, D., Janovick, J. A., Brothers, S., and Conn, P. M. (1997) *Mol. Endocrinol. 11*, 738−746.
12. Stanislaus, D., Ponder, S., Ji, T. H., and Conn, P. M. (1998) *Biol. Reprod. 59*, 579−586.
13. Palczewski, K., Kumasaka, T., Hori, T., Behnke, C. A., Motoshima, H., Fox, B. A., Le Trong, I., Teller, D. C., Okada, T., Stenkamp, R. E., Yamamoto, M., and Miyano, M. (2000) *Science 289*, 739−745.
14. Schwartz, T. W. (1994) *Curr. Opin. Biotechnol. 5*, 434−444.
15. Flanagan, C. A., Rodic, V., Konvicka, K., Yuen, T., Chi, L., Rivier, J. E., Millar, R. P., Weinstein, H., and Sealfon, S. C. (2000) *Biochemistry 39*, 8133−8141.
16. Zhou, W., Rodic, V., Kitanovic, S., Flanagan, C. A., Chi, L., Weinstein, H., Maayani, S., Millar, R. P., and Sealfon, S. C. (1995) *J. Biol. Chem. 270*, 18853−18857.
17. Davidson, J. S., McArdle, C. A., Davies, P., Elario, R., Flanagan, C. A., and Millar, R. P. (1996) *J. Biol. Chem. 271*, 15510−15514.
18. Flanagan, C. A., Becker, I. I., Davidson, J. S., Wakefield, I. K., Zhou, W., Sealfon, S. C., and Millar, R. P. (1994) *J. Biol. Chem. 269*, 22636−22641.
19. Hoffmann, S. H., ter Laak, T., Kühne, R., Reiländer, H., and Beckers, T. (2000) *Mol. Endocrinol. 14*, 1099−1115.
20. Chauvin, S., Bérault, A., Lerrant, Y., Hibert, M., and Counis, R. (2000) *Mol. Pharmacol. 57*, 625−633.
21. Layman, L. C., Cohen, D. P., Jin, M., Xie, J., Li, Z., Reindollar, R. H., Bolbolan, S., Bick, D. P., Sherins, R. R., Duck, L. W., Musgrove, L. C., Sellers, J. C., and Neill, J, D. (1998) *Nat. Genet. 18*, 14−15.
22. de Roux, N., Young, J., Brailly-Tabard, S., Misrahi, M., Milgrom, E., and Schaison, G. (1999) *J. Clin. Endocrinol. Metab. 84*, 567−572.
23. Myburgh, D. B., Pawson, A. J., Davidson, J. S., Flanagan, C. A., Millar, R. P., and Hapgood, J. P. (1998) *Eur. J. Endocrinol. 139*, 438−447.
24. Ausubel, F. M., Brent, R., Kingston, R. E., Moore, D. D., Seidman, J. G., Smith, J. A., and Struhl, K. (1989) in *Current protocols in molecular biology*, J. Wiley & Sons, New York.
25. Ballesteros, J., Kitanovic, S., Guarnieri, F., Davies, P., Fromme, B. J., Konvicka, K., Chi, L., Millar, R. P., Davidson, J. S.,

Weinstein, H., and Sealfon, S. C. (1998) *J. Biol. Chem. 273*, 10445−10453.
26. Flanagan, C. A., Zhou, W., Chi, L., Yuen, T., Rodic, V., Robertson, D., Johnson, M., Holland, P., Millar, R. P., Weinstein, H., Mitchell, R., and Sealfon, S. C. (1999) *J. Biol. Chem. 274*, 28880−28886.
27. Davidson, J. S., Assefa, D., Pawson, A., Davies, P., Hapgood, J., Becker, I., Flanagan, C., Roeske, R., and Millar, R. P. (1997) *Biochemistry 36*, 12881−12889.
28. Case, D. A., Pearlman, D. A., Cladwell, J. W., Chaetham, T. E., III, Ross, W. S., Simmerling, C. L., Darden, T. A., Merz, K. M., Stanton, R. V., Cheng, A. L., Vincent, J. J., Crowley, M., Tsui, V., Radmer, R. J., Duan, Y., Pitera, J., Massova, I., Seibel, G. L., Singh, U. C., Weiner, P. K., and Kollman, P. A. (1998) *AMBER 5*, University of California, San Francisco, CA.
29. ter Laak, A. M., and Kühne, R. (1999) *Recept. Channels 6*, 295−308.
30. Beckers, T., Marheineke, K., Reiländer, H., and Hilgard, P. (1995) *Eur. J. Biochem. 231*, 535−543.
31. Kaiser, U. B., Zhao, D., Cardona, G. R., and Chin, W. W. (1992) *Biochem. Biophys. Res. Commun. 189*, 1645−1652.
32. Kakar, S. S., Musgrove, L. C., Devor, D. C., Sellers, J. C., and Neill, J. D. (1992) *Biochem. Biophys. Res. Commun. 189*, 289−295.
33. Davidson, J. S., Flanagan, C. A., Zhou, W., Becker, I. I., Elario, R., Emeran, W., Sealfon, S. C., and Millar, R. P. (1995) *Mol. Cell. Endocrinol. 107*, 241−245.
34. Chi, L., Zhou, W., Prikhozhan, A., Flanagan, D., Davidson, K. J. S., Golembo, M., Illing, N., Millar, R. P., and Sealfon, S. C. (1993) *Mol. Cell. Endocrinol. 91*, R1−R6.
35. Cook, J. V., and Eidne, K. A. (1997) *Endocrinology 138*, 2800−2806.

BI0113162